# Membrane associated complexes in calcium dynamics modelling



2013 Phys. Biol. 10 035004

(http://iopscience.iop.org/1478-3975/10/3/035004)

Phys. Biol. **10** (2013) 035004 (13pp) doi:10.1088/1478-3975/10/3/035004

# Membrane associated complexes in calcium dynamics modelling

**Piotr Szopa**[1,2], **Michał Dyzma**[1] **and Bogdan Kaźmierczak**[1]

[1] Institute of Fundamental Technological Research, Polish Academy of Sciences, Warsaw, Poland
[2] Faculty of Mathematics, Informatics and Mechanics, University of Warsaw, Poland

E-mail: bkazmier@ippt.gov.pl

Received 13 January 2013
Accepted for publication 15 February 2013
Published 4 June 2013
Online at stacks.iop.org/PhysBio/10/035004

**Abstract**
Mitochondria not only govern energy production, but are also involved in crucial cellular signalling processes. They are one of the most important organelles determining the $Ca^{2+}$ regulatory pathway in the cell. Several mathematical models explaining these mechanisms were constructed, but only few of them describe interplay between calcium concentrations in endoplasmic reticulum (ER), cytoplasm and mitochondria. Experiments measuring calcium concentrations in mitochondria and ER suggested the existence of cytosolic microdomains with locally elevated calcium concentration in the nearest vicinity of the outer mitochondrial membrane. These intermediate physical connections between ER and mitochondria are called MAM (mitochondria-associated ER membrane) complexes. We propose a model with a direct calcium flow from ER to mitochondria, which may be justified by the existence of MAMs, and perform detailed numerical analysis of the effect of this flow on the type and shape of calcium oscillations. The model is partially based on the Marhl *et al* model. We have numerically found that the stable oscillations exist for a considerable set of parameter values. However, for some parameter sets the oscillations disappear and the trajectories of the model tend to a steady state with very high calcium level in mitochondria. This can be interpreted as an early step in an apoptotic pathway.

## 1. Calcium homeostasis

Cells maintain over 10 000-fold ratio between cytosolic (0.1–1 $\mu$M) and extracellular (2 mM) calcium concentrations [1]. The $Ca^{2+}$ level inside the cell differs also significantly between specific cell organelles, i.e. mitochondria (0.2–500 $\mu$M), endoplasmic reticulum (ER) (100–500 $\mu$M) or nucleus (0.1–2 $\mu$M) [2].

Calcium homeostasis is sustained by pumps, channels, exchangers and buffer proteins governing specific fluxes. A plasma membrane $Ca^{2+}$ ATPase pumps and $Na^{+}/Ca^{2+}$ exchangers (NCX) actively remove $Ca^{2+}$ from the cytosol into the extracellular space. Sarco-endoplasmic reticulum $Ca^{2+}$ ATPase (SERCA) pumps calcium from the cytosol to the lumen of ER, while $IP_3R$ or ryanodine receptors (RyR) release calcium from these stores. Voltage-dependent anion channels (VDAC) of the outer mitochondrial membrane (OMM) and uniporters on the internal mitochondrial membrane (IMM) allow $Ca^{2+}$ to reach the mitochondrial matrix along the electro-chemical gradient [3, 4]. $Ca^{2+}$ ions can exit mitochondria through specific sodium–calcium exchangers (MNCX) located on the IMM, which remove calcium from the matrix to the perimitochondrial space, by replacing it with sodium ions with 1:3 ratio [5]. The calcium ions exit the perimitochondrial space either through VDAC channels or by transmembrane diffusion. Under specific conditions, when mitochondria uptake vast amount of calcium, it may be released by specific mitochondrial permeability transition pores (PTPs). According to [6, 7], the opening of PTPs is the crucial step occurring in the very beginning of the apoptotic pathway [8] which inevitably directs the cell to a programmed death. This process results in many irreversible physical changes in mitochondria and consequently in the whole cell which cannot be described in our relatively simple model. (The more precise description of these changes is provided in section 4.) That is why, we confine ourselves only to analysing the processes preceding the PTPs opening, which is rapid mitochondrial calcium uptake and 'mitochondrial swelling'.

 

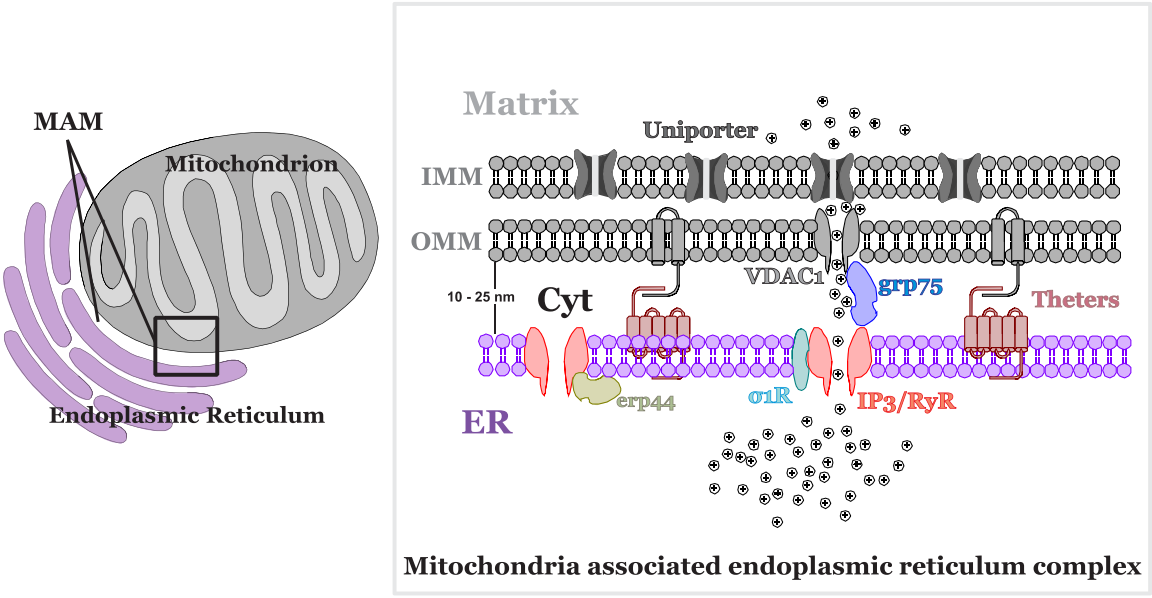


**Figure 1.** Mitochondria-associated ER membrane complex (MAM), ER—endoplasmic reticulum, Cyt—cytosol, $IP_3R$/RyR—calcium channels on the surface of the ER, VDAC-1/uniporter—calcium channels on outer mitochondria membrane, erp44/erp57—endoplasmic reticulum protein 44/57, $\sigma_1$R—sigma-1 receptor and grp75 chaperone.

In this paper, we will analyse this phenomenon within the mathematical model taking into account the mitochondria-associated ER complexes.

## 2. Mitochondria-associated endoplasmic reticulum complexes

The existence of a physical interface between ER and mitochondria was first reported by Dennis and Kennedy, who described membrane fraction, isolated from rat hepatocytes and tested for mitochondrial and reticular enzymes [9]. Later it was identified to be involved in lipids' metabolism [10]. Recent experiments demonstrated that mitochondria and ER indeed form functional complexes with each other [11] functioning as hubs for lipid metabolism, calcium signalling and apoptosis. Proximity between membranes may lead to a spontaneous aggregation of specific chaperones and peptidic tethers which keep channel proteins and other transmembrane elements of the ER and OMM in close contact. These complexes are known as the mitochondria-associated ER membrane complexes (MAMs) [12]. A scheme and an electron micrograph of the MAM are presented in figures 1 and 2. The distance between membranes in MAMs was estimated using electron tomography. It ranges from 10 nm for smooth ER to 25 nm for rough ER [13]. Appositions of the ER and OMM are stabilized by several proteins, including $Ca^{2+}$ channels VDAC-1 and $IP_3R$ type-3/RyR, sigma-1 receptor chaperone and autocrine motility factor receptor, forming an ER–mitochondria interface. Molecular chaperones such as glucose-regulated protein link physically VDAC-1 and $IP_3$R/RyR. Several other proteins, such as calreticulin, calnexin, ERp44, ERp57, the cytosolic sorting protein and other peptidic tethers, bind membranes together and stabilize the area of interaction either on the ER or mitochondrial side [14].

These sites of close contact are also described as 'hot spots' or microdomains, where calcium concentration reaches much higher values required for uniporter activation. Microdomains existence was postulated for a long time, but there was no experimental confirmation. Csordas [15] and Giacomello [16] measured changes of calcium concentration upon $IP_3$ activation in these specific structures using modified fluorescent probes targeted at the reticulum surface. Their results indicate that during stimulation, calcium concentration in microdomains is five to tenfold higher than that in the bulk cytosol and may reach up to 9 $\mu$M. Proximity between organelles and partial isolation from the rest of the cell leads to the rapid changes of the calcium level and allows 'direct' flow of $Ca^{2+}$ from ER to mitochondria.

In contrast to prior papers, modelling whole cell calcium dynamics [17–21], we introduce an additional flux directly from the ER to mitochondria. According to [22], 90% of ER calcium release units ($IP_3$R/RYR) are located close to mitochondria and the majority of mitochondrial calcium uptake sites (uniporters) sense the high calcium concentration in the vicinity of reticular calcium release sites. Additionally, we included in our model two modes of uniporter activity, which are rapid uptake mode (RaM) and classical uniporter mode (see section 3).

## 3. The model

The models proposed in [18–20] and [21] describe the evolution of calcium in three specified cellular compartments: ER, mitochondria and cytosol. The cytosolic calcium level depends on fluxes across the ER membrane, mitochondria membrane and binding of free $Ca^{2+}$ to cytosolic buffer proteins (see table 1; [23–25]). Moreover in the above models, the exchange of calcium between the ER and the mitochondria is only via cytosol.

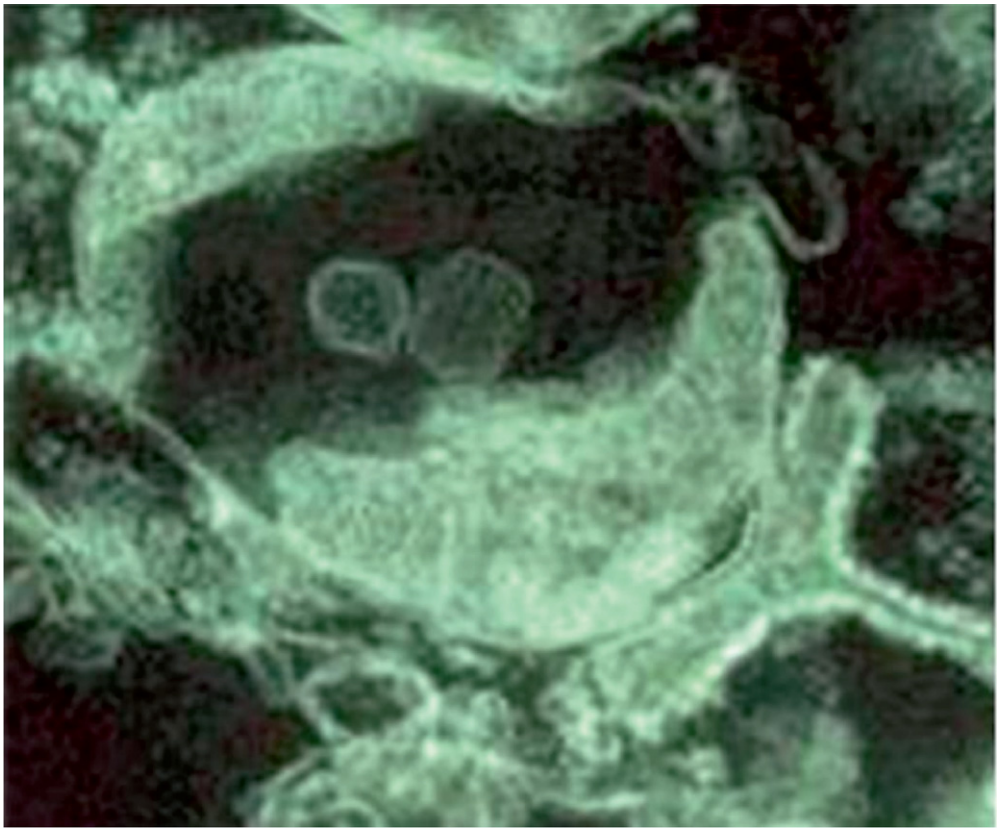

**Figure 2.** Mitochondria-associated ER membrane complex (MAMs)—electron micrograph (by Mariusz R Wieckowski).

**Table 1.** Calcium buffers in specific cellular compartments.

| Cytosol | Endoplasmic reticulum | Mitochondria |
|---|---|---|
| Calmodulin | Calreticulin | Phosphate |
| Calretinin | Grp94 | MICU 1 |
| Calbindin-D28k | BiP/Grp78 | |
| Calbindin-D9k | Calnexin | |
| Parvalbumin $\alpha$ | ERp72 | |
| Parvalbumin $\beta$ | PDI/calcistorin | |

We propose a model, which may be regarded as a modification of the model from [19], with an alternative approach to the mitochondrial calcium dynamics. In our approach, we divide the calcium influx to mitochondria into two parts: flux through mitochondrial calcium uniporters (MCU) located in MAMs ($J_{\mathrm{MAM}}$) sensing elevated $Ca^{2+}$ concentration (assumed to be equal to that in ER), and flux through uniporters located outside MAMs ($J_{\mathrm{in}}$) sensing bulk cytosolic calcium concentration. Moreover, we consider the uniporter working in two modes: standard uniporter mode, described by the Hill function with a Hill coefficient equal to 2 [26], and RaM, discovered in the 1990s [27], modelled by the Hill function with a high Hill coefficient [28]. We also modify the calcium efflux from mitochondria. In the presented model, this flow depends only on the mitochondrial calcium level, whereas in [19] the speed of the calcium outflow from the mitochondria to cytosol is determined also by cytosolic calcium concentration.

It is worthwhile to note that in previous models the MAMs' influence on the mitochondria calcium fluxes has been considered implicitly. To be more precise, in the papers of Marhl [18, 19] mitochondrial calcium uptake was described by a Hill function depending on cytosolic calcium concentration; however, elevated calcium concentration at MAMs was modelled by taking relatively small half-activation constant (0.7 $\mu$M) and a high Hill coefficient equal to 8. As stated in Marhl *et al*, such a choice was dictated by experiments showing a fast calcium flux into mitochondria at free cytosolic calcium concentration of about 0.5–1.0 $\mu$M, and by the fact that the MCU is not effective at low cytosolic calcium concentrations [29–32].

A schematic representation of our model is depicted in figure 3. We use a system of ODEs to describe the evolution of calcium concentrations in different cellular compartments. Such a description is not strictly legitimate, due to the fact that the effective diffusion coefficient of free calcium ions ($\approx$300 $\mu m^2\,s^{-1}$) decreases significantly in the presence of buffer molecules [17]. Thus, the local in space concentration of calcium ions may not equalize within times negligible in comparison with the periods of considered oscillations. However, despite the additional fact that the calcium channels form clusters distributed non-homogeneously on the membranes of ER [33] and mitochondria [34, 35], and the fact that the mitochondria themselves may be gathered in the parts of the cell which require more intensive energy supply, in works dealing with intracellular calcium oscillations, it is common practice to neglect the non-homogeneities of calcium distribution and to describe the evolution of the spatially averaged concentration

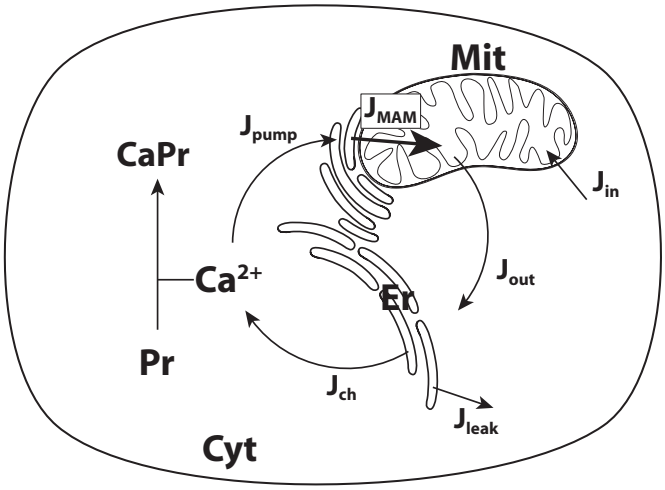


**Figure 3.** Schematic representation of the model: ER—endoplasmic reticulum, Mit—mitochondrion, Cyt—cytosol.

of calcium in different compartments by ODEs (see e.g. [26] and references therein).

Another problem in applying spatially homogeneous models described by ODEs is a stochastic nature of a single calcium channel activity which takes the form of irregular opening events called 'blips'. This can further lead to a stochastic activation of other channels within the same cluster (called 'puffs') [33]. However, in cells with large population of channels bursting may occur in a quasi-synchronized manner in response to sufficiently strong external stimulus; thus, it may be justified to use spatially homogeneous models [36].

In our model, the concentrations of free calcium ions in the cytosol ($Ca_{Cyt}$), endoplasmic reticulum ($Ca_{ER}$) and mitochondria ($Ca_{Mit}$) as well as the concentration of calcium ions bound to buffer proteins in the cytosol (CaPr) and the concentration of free binding sites of the cytosolic buffer proteins (Pr) are subject to the following equations:

$$\frac{dCa_{Cyt}}{dt} = J_{ch} + J_{leak} - J_{pump} + J_{out} - J_{in} + k_{-}CaPr - k_{+}Ca_{Cyt}Pr, \quad (1)$$

$$\frac{dCa_{ER}}{dt} = \frac{\beta_{ER}}{\rho_{ER}}(J_{pump} - J_{ch} - J_{leak} - J_{MAM}), \quad (2)$$

$$\frac{dCa_{Mit}}{dt} = \frac{\beta_{Mit}}{\rho_{Mit}}(J_{in} + J_{MAM} - J_{out}), \quad (3)$$

$$\frac{dCaPr}{dt} = k_{+}Ca_{Cyt}Pr - k_{-}CaPr, \quad (4)$$

$$\frac{dPr}{dt} = -k_{+}Ca_{Cyt}Pr + k_{-}CaPr, \quad (5)$$

where $k_+$ and $k_-$ denote the average kinetic constants of $Ca^{2+}$ binding to the buffer proteins and the reverse process, respectively. The coefficients $\rho_{ER}$ and $\rho_{Mit}$ denote the volume ratio between the ER and the cytosol, and between the mitochondria and the cytosol, respectively. We assume that calcium sequestration in the ER and the mitochondria by buffers is very fast, much faster than the fluxes to and from these cellular compartments [31, 37–39]; therefore, for simplicity, we use the quasi-steady state approximation, i.e. we assume (as in [19]) that the ratio of the concentrations of free calcium in the ER and mitochondria to the respective total concentration of calcium (free and buffered) is constant and equal to $\beta_{ER}$ and $\beta_{Mit}$, respectively. We assume that there is no calcium exchange between the cell and the extracellular space. This assumption can be justified because it is often the case that the calcium transport across the cell membrane is much slower than the calcium transport to and from the internal compartments; thus, the total amount of calcium in the cell can be treated as a slowly varying magnitude [40]. Moreover, according to [40], even if transport across the plasma membrane is blocked, oscillations can still occur, provided that the total amount of $Ca^{2+}$ in the cell is in a proper range. Consequently, we have the following conservation relation for the total amount of calcium:

$$Ca_{tot} = Ca_{Cyt} + \frac{\rho_{ER}}{\beta_{ER}}Ca_{ER} + \frac{\rho_{Mit}}{\beta_{Mit}}Ca_{Mit} + CaPr. \quad (6)$$

Moreover, adding equations (4) and (5) we obtain $\frac{d}{dt}(CaPr + Pr) = 0$, which implies that the total concentration $Pr_{tot}$ of calcium binding sites (i.e. those with calcium ions bound and those with no calcium ions bound) is constant, that is to say

$$Pr(t) + CaPr(t) = Pr_{tot}(t) = Pr_{tot}(0) = Pr(0) + CaPr(0). \quad (7)$$

Thus, by means of the conservation relations (6) and (7), the system of equations (1)–(5) may be reduced to a three-dimensional one, which reads

$$\frac{dCa_{Cyt}}{dt} = J_{ch} + J_{leak} - J_{pump} + J_{out} - J_{in} + k_{-}CaPr - k_{+}Ca_{Cyt}(Pr_{tot} - CaPr), \quad (8)$$

$$\frac{dCa_{ER}}{dt} = \frac{\beta_{ER}}{\rho_{ER}}(J_{pump} - J_{ch} - J_{leak} - J_{MAM}), \quad (9)$$

$$\frac{dCa_{Mit}}{dt} = \frac{\beta_{Mit}}{\rho_{Mit}}(J_{in} + J_{MAM} - J_{out}), \quad (10)$$

where

$$CaPr = Ca_{tot} - Ca_{Cyt} - \frac{\rho_{ER}}{\beta_{ER}}Ca_{ER} - \frac{\rho_{Mit}}{\beta_{Mit}}Ca_{Mit}. \quad (11)$$

The active influx of $Ca^{2+}$ into the ER lumen $J_{pump}$ performed by SERCA pumps and the effluxes $J_{ch}$ and $J_{leak}$ from this compartment are given by (see [19])

$$J_{pump} = k_{pump}Ca_{Cyt}, \quad (12)$$

$$J_{ch} = k_{ch}\frac{Ca_{Cyt}^2}{K_1^2 + Ca_{Cyt}^2}(Ca_{ER} - Ca_{Cyt}), \quad (13)$$

$$J_{leak} = k_{leak}(Ca_{ER} - Ca_{Cyt}). \quad (14)$$

$J_{pump}$ depends directly on cytoplasmic $Ca^{2+}$ concentration with $k_{pump}$ as a rate constant of the pump. Calcium ions may exit the ER lumen via $IP_3R$/RyR channels ($J_{ch}$). This flow depends on the concentration gradient ($Ca_{ER} - Ca_{Cyt}$); $k_{ch}$ denotes the maximal permeability of the channels. The Hill function in the expression for $J_{ch}$ represents the CICR (calcium-induced calcium release) mechanism and $K_1$ is the half-activation constant. We also consider the non-specific leak flux $J_{leak}$, the driving force of which is the concentration gradient across the

ER membrane; $k_{leak}$ denotes the rate constant for $Ca^{2+}$ leakage through the membrane of the ER.

The mitochondrial calcium dynamics is determined by the following fluxes:

$$J_{out} = k_{out}\frac{Ca_{Mit}}{K_3 + Ca_{Mit}} \tag{15}$$

$$J_{in} = J_{in2} + J_{in8} := k_{in2}\frac{Ca^2_{Cyt}}{K^2_{2,2} + Ca^2_{Cyt}} + k_{in8}\frac{Ca^8_{Cyt}}{K^8_{2,8} + Ca^8_{Cyt}}, \tag{16}$$

$$J_{MAM} = J_{MAM2} + J_{MAM8} := k_{MAM2}\frac{Ca^2_{ER}}{K^2_{4,2} + Ca^2_{ER}} + k_{MAM8}\frac{Ca^8_{ER}}{K^8_{4,8} + Ca^8_{ER}}. \tag{17}$$

The slow calcium release from the mitochondria takes place through $Na^+/Ca^{2+}$ and $H^+/Ca^{2+}$ exchangers. This flow has only minimal influence on the transmembrane potential $\Delta\Psi_m$ (section 3.4 in [26, 41]); thus, the changes in $\Delta\Psi_m$ are neglected in the model formulation. We express the calcium efflux from the mitochondria $J_{out}$ as given above according to [42]; however, we neglect the dependence on the concentration of $Na^+$ ions. To be more precise, we replace the Hill function $Na^2_{Cyt}/(K^2_{MCX,NA} + Na^2_{Cyt})$ by its average over the period of oscillations. $k_{out}$ stands for the maximal rate of calcium flow through $Na^+/Ca^{2+}$ and $H^+/Ca^{2+}$ exchangers and $K_3$ is the half-activation constant.

As we mentioned above, the calcium flow into the mitochondria takes place through MCU [43]. It is hypothesized [28, 44] that MCU can work in the two modes: usual uniporter mode and RaM. The calcium flow in the usual uniporter mode is described by the Hill function with a Hill coefficient equal to 2 [26]. The rapid uptake mode may be 'constructed on demand' by conformational changes of the uniporter complex [28]. According to [28], calcium flow through RaM can be described by the Hill function with a very high Hill coefficient (we set this exponent to 8 in this paper). The precise form of the flux through uniporters depends on whether they are located outside or inside the MAM complexes.

As is mentioned in [22], the majority of ER calcium release units ($IP_3$Rs/RyRs) are placed in sites of close contact of ER and mitochondria. Likewise, the majority of the calcium uniporters distributed on the IMM are located in the regions of close proximity of the ER and the OMM (see figure 2), thus creating MAMs [12]. MAM-situated MCU sense high local calcium concentration occurring in the vicinity of reticular calcium release sites. According to these facts, we have decided to divide the mitochondrial calcium influx into two parts: $J_{in}$, describing the calcium flow through uniporters located outside the MAM interface, and $J_{MAM}$, describing the flow through the uniporters located within MAMs. The intensity of the $J_{in}$ flow is regulated by the bulk cytosolic calcium concentration $Ca_{Cyt}$. Due to the fact that MAMs have very small volume and are separated from the rest of the cell, it will be assumed in the paper that the intensity of $J_{MAM}$ is regulated by the calcium concentration in the endoplasmic reticulum $Ca_{ER}$ [15]; thus calcium influx through these uniporters can be regarded as a straightforward flow from the ER to the mitochondria.

The MCU is driven by the electrochemical gradient across the IMM, denoted as $\Delta\Psi_m$ (cf [43]). The value of a transmembrane potential $\Delta\Psi_m$ which gives rise to this flow is implicitly taken into account in both $k_{in2}$ and $k_{in8}$. In our model, we will assume that $\Delta\Psi_m = \text{const}$ due to the fact that the only factor able to change the transmembrane potential $\Delta\Psi_m$ is the massive efflux of the matrix contents (in particular $Ca^{2+}$ ions) through PTPs. Although some papers consider the outflow of calcium through PTPs in low conductance state [4, 19], it seems that PTPs' opening takes place extremely rarely and mainly under stress conditions when an apoptotic process is activated [45]. Thus, the possible flow through PTPs is not taken into account.

Due to what was mentioned above, the total calcium flux from the cytosol to mitochondria is divided into two parts: one corresponding to the usual uniporter mode proportional to maximal permeability $k_{in2}$ and the other one corresponding to the rapid mode with maximal permeability $k_{in8}$. $K_{2,2}$ denotes the half-activation constant for the free cytosolic calcium in the usual mode. There is no agreement in the literature with respect to the values of $K_{2,2}$, which range from 1 to 189 $\mu$M [46]; therefore, we set $K_{2,2}$ equal to 20. Similarly, $K_{2,8}$ denotes the RaM mode half-activation constant. In this mode, uniporter is very fast and effective for an external calcium level higher than about 0.5 $\mu$M (cf [26, 30]).

As mentioned above, the main objective of this paper is to incorporate explicitly into a mathematical model the existence of regions of very close proximity of ER and mitochondria (MAMs), implying the possibility of the straightforward flux of the free calcium ions from the ER to the mitochondria.

The constants $k_{MAM2}$, $k_{MAM8}$ and $K_{4,2}$, $K_{4,8}$ denote the maximal permeability and half-activation constants for uniporter's usual and RaM mode in the $J_{MAM}$ flux. Since the calcium is taken up by the mitochondria through the same type of uniporters regardless of the presence of ER in the neighbourhood of the OMM, we postulate $J_{MAM}$ to have the same form as $J_{in}$, i.e. the same Hill coefficients. However, due to the close proximity of uniporters to the ER, we will assume below that the permeability of the MAM's uniporters depends straightforwardly on the free calcium concentration in endoplasmic reticulum $Ca_{ER}$ (see [16] and [22], p 72). This is the main quantitative difference between $J_{in}$ and $J_{MAM}$. As shown in the left panel of figure 6, the calcium flow through MAM interfaces plays a significant role in the calcium dynamics in our model.

The values of $\beta_{ER}$, $\beta_{Mit}$, $\rho_{ER}$ and $\rho_{Mit}$ in table 2 are taken from [19] (see also [47]). These parameters depend on the type of cells considered. However, as it is seen, only the ratios of these coefficients are essential. To fix our attention, we will assume throughout the paper that $\beta_{ER}/\rho_{ER}$ and $\beta_{Mit}/\rho_{Mit}$ are equal to 0.25.

## 4. Analysis of the model

First, we show the basic mathematical properties of the model, that is, the existence and uniqueness of non-negative

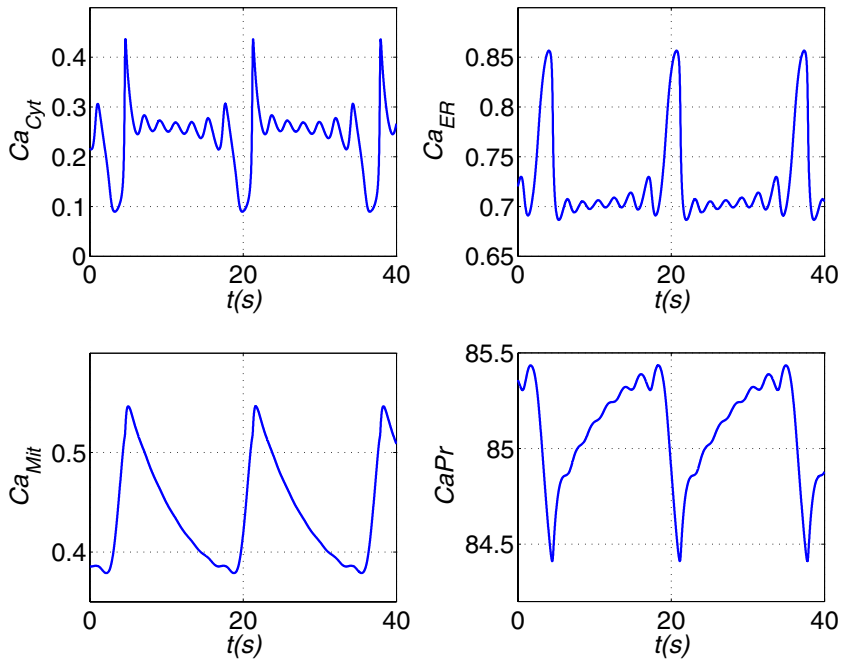


**Figure 4.** Trajectories of calcium concentration in specific compartments: bursting oscillations. Parameters as in table 2.

**Table 2.** The parameters of the model.

| Parameter | Value | Parameter | Value |
|---|---|---|---|
| Concentrations | | Ratios of volumes | |
| $Ca_{tot}$ | 90 $\mu$M | $\rho_{ER}$ | 0.01 |
| $Pr_{tot}$ | 120 $\mu$M | $\rho_{Mit}$ | 0.01 |
| Kinetic parameters | | Ratios of concentrations | |
| $k_{ch}$ | 4200 $s^{-1}$ | $\beta_{ER}$ | 0.0025 |
| $k_{pump}$ | 20 $s^{-1}$ | $\beta_{Mit}$ | 0.0025 |
| $k_{leak}$ | 0.05 $s^{-1}$ | | |
| $k_{in2}$ | 20 $\mu$M $s^{-1}$ | Half-activation constants | |
| $k_{in8}$ | 80 $\mu$M $s^{-1}$ | $K_1$ | 5 $\mu$M |
| $k_{MAM2}$ | 50 $\mu$M $s^{-1}$ | $K_{2,2}$ | 20 $\mu$M |
| $k_{MAM8}$ | 200 $\mu$M $s^{-1}$ | $K_{2,8}$ | 0.8 $\mu$M |
| $k_+$ | 0.1 $\mu M^{-1} s^{-1}$ | $K_3$ | 3.1 $\mu$M |
| $k_-$ | 0.01 $s^{-1}$ | $K_{4,2}$ | 20 $\mu$M |
| $k_{out}$ | 1.9 $\mu$M $s^{-1}$ | $K_{4,8}$ | 1.8 $\mu$M |

global solutions. Next, we perform the numerical analysis. We examine the existence and stability of steady states, existence, period and type (regular or bursting) of calcium oscillations. By *bursting* oscillations we understand the oscillations which are characterized by the superposition of the low-amplitude high-frequency and high-amplitude low-frequency oscillations (see the upper panels of figure 4).

Due to the structure of the model, the following existence theorem holds.

**Theorem 1.** *Assume that* $Ca_{Cyt}(0)$, $Ca_{ER}(0)$, $Ca_{Mit}(0)$, $CaPr(0)$ *and* $Pr(0)$ *are non-negative. Then the solutions to equations (1)–(5) are unique, global in time and non-negative.*

The non-negativity of solutions is important from the biological point of view, because concentrations cannot become negative. The proof of this theorem is a simply consequence of the below lemma.

**Lemma 1.** *(Proposition 1.1 in [48]) The cone* $\mathbb{R}^N_+$ *is invariant for the flow generated by the equation*

$$\frac{du}{dt} = F(u)$$

*if an only if the function* $F(u)$ *is quasi-positive, i.e. for every* $i = 1, \ldots, N$ *the function*

$$F_i(u_1, \ldots, 0, \ldots, u_N) \geqslant 0,$$

*where* 0 *stands at the ith position and* $u_j \geqslant 0$ *for* $j \neq i$.

**Proof.** First, using lemma 1, we prove the non-negativity of solutions. Then, we prove the boundedness and thus the global existence.

In our case, $N = 5$ and

$$F_1(0, Ca_{ER}, Ca_{Mit}, CaPr, Pr) = k_{leak}Ca_{ER} + k_{out}\frac{Ca_{Mit}}{K_3 + Ca_{Mit}} + k_-CaPr,$$

$$F_2(Ca_{Cyt}, 0, Ca_{Mit}, CaPr, Pr) = \frac{\beta_{ER}}{\rho_{ER}}\left(k_{pump}Ca_{Cyt} + k_{ch}\frac{Ca_{Cyt}^3}{K_1^2 + Ca_{Cyt}^2} + k_{leak}Ca_{Cyt}\right),$$

$$F_3(Ca_{Cyt}, Ca_{ER}, 0, CaPr, Pr) = \frac{\beta_{Mit}}{\rho_{Mit}}\left(k_{in}\frac{Ca_{Cyt}^8}{K_2^8 + Ca_{Cyt}^8} + k_{MAM}\frac{Ca_{ER}^8}{K_4^8 + Ca_{ER}^8}\right),$$

$$F_4(Ca_{Cyt}, Ca_{ER}, Ca_{Mit}, 0, Pr) = k_+Ca_{Cyt}Pr,$$

$$F_5(Ca_{Cyt}, Ca_{ER}, Ca_{Mit}, CaPr, 0) = k_-CaPr.$$

The above functions are obviously non-negative for non-negative $Ca_{Cyt}$, $Ca_{Mit}$, $Ca_{ER}$, CaPr and Pr; thus, the solutions are non-negative. We consider a cell as an isolated system, i.e. there are no fluxes between the cell volume and the extracellular space. It follows from the conservation of total $Ca^{2+}$ amount (6) and non-negativity of solutions that $Ca_{Cyt}(t)$,

$\frac{\rho_{ER}}{\beta_{ER}}Ca_{ER}(t)$ and $\frac{\rho_{Mit}}{\beta_{Mit}}Ca_{Mit}(t)$ are bounded above by $Ca_{tot}$, while Pr(t) and CaPr(t) are bounded above by $Pr_{tot}$. The functions $F_1$–$F_5$ are polynomials or rational functions with denominators separated from 0, thus satisfying the local Lipschitz condition. It follows that the solutions to system (1)–(5) are global in time and unique. □

For all simulations, unless stated otherwise, we have used the values of parameters given in table 2. It is also convenient to define the parameter

$$k_{MAM} = k_{MAM2} + k_{MAM8}.$$

We also fix the ratio as

$$k_{MAM8}/k_{MAM2} = 4.$$

Below, we will analyse the following properties of the considered model.

(1) Existence of bursting oscillations in the system.
(2) Steady states, limit cycles and impact of $k_{MAM}$ on calcium levels.
(3) Effect of MAMs on the period of oscillations.
(4) Possible scenario of apoptosis.

We have investigated our model by numerical integration of the model equations using the MATLAB software. We have used the 3D version of the model equations, i.e. equations (8)–(10), but in some figures we have depicted additionally time courses of CaPr.

The stationary points of the system (8)–(10) were found by the use of the MATLAB optimization toolbox for the parameter set as in table 2 and then continued with respect to $k_{MAM}$ by means of MatCont (MATLAB continuation toolbox) [49]. We have found the bursting type of calcium oscillations for different sets of model parameters. Moreover, we have found sets of parameters for which after a transient time of oscillations, the system approaches a steady state with a relatively high mitochondrial calcium level. This can be interpreted as an early step in an apoptotic pathway consisting in sequestering large amount of calcium in mitochondria and the subsequent opening of the PTPs (see [8, 50–52]). This phenomenon will be described in more detail below (point 'Possible scenario of apoptosis').

As it is seen from the time courses of mitochondrial calcium influxes for bursting oscillations with parameters as in table 2 (the left panel of figure 6), the fluxes through MAM structures play a significant role in the calcium dynamics described by the model. Although the maximal values of the flux $J_{in}$ are slightly higher than those of $J_{MAM}$, the total flux through MAM structures $\int_t^{t+T} J_{MAM}(s)\,ds = 3.55$ over one period with $T = 16.65$ s is larger than the total flux through uniporters situated outside the MAM interface $\int_t^{t+T} J_{in}(s)\,ds = 0.37$. In the right panel of figure 6, we have depicted the time courses of the two parts of $J_{MAM}$: the usual uniporter mode $J_{MAM2}$ and the rapid mode $J_{MAM8}$ (defined in (17)). The maximal values of $J_{MAM2}$ are smaller than those of $J_{MAM8}$ and the total flux in usual mode $\int_t^{t+T} J_{MAM2}(s)\,ds = 1.08$ is much smaller than the total flux in the rapid mode $\int_t^{t+T} J_{MAM8}(s)\,ds = 2.47$. Thus, the rapid mode is important in shaping the calcium oscillations.

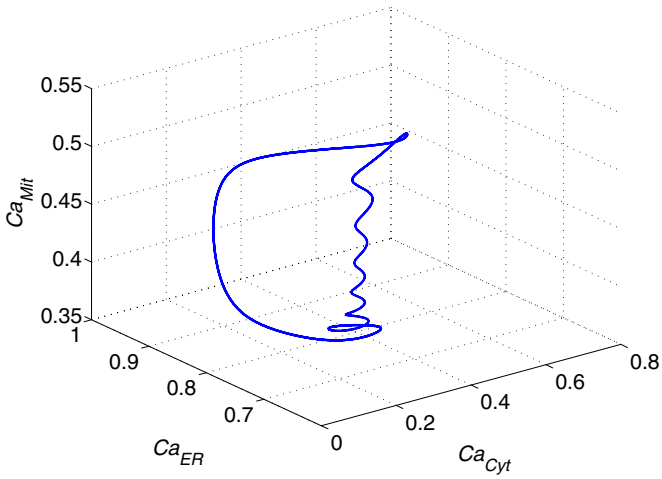


**Figure 5.** 3D phase portrait of bursting calcium oscillations. Parameters as in table 2.

(1) *Existence of bursting oscillations in the system.* The plots of time changes of concentration of $Ca^{2+}$ ions in specific compartments for the parameter set as in table 2 are given in figure 4. In figure 5, we present the 3D-phase portrait of the limit cycle for the same parameters as in figure 4. The bursting calcium oscillations presented in figure 5 can be described approximately as a slow calcium efflux from mitochondria and the fast exchange of calcium between cytosol and ER. One period of bursting calcium oscillations is presented in figure 7. The cycle can be divided into three phases.

Phase I begins when the level of cytosolic calcium ($Ca_{Cyt}$) reaches its maximal value ($t = 4.4$) and continues until the calcium level in mitochondria ($Ca_{Mit}$) reaches its maximal value ($t = 4.8$). In this phase, the leading processes are the release of $Ca^{2+}$ ions from ER and the uptake of calcium ions by mitochondria and cytosolic buffer proteins.

In phase II, the slow flux of calcium from mitochondria to cytosol takes place. The majority of released calcium is bound by cytosolic buffer proteins. The second process during this phase is the fast calcium exchange between the cytosol and ER, which results in small, fast oscillations of calcium levels in these compartments. This phase ends when the level of buffered calcium (CaPr) reaches maximum ($t = 18.1$).

In phase III, the leading process is the dissociation of calcium–protein complexes. The mitochondria and ER are being loaded, while the calcium level in cytosol first decreases and then increases to reach the maximal value, which is the end of phase III ($t = 21.05$). The whole period lasts 16.65 s and the values of free calcium concentrations in particular compartments are $Ca_{Cyt} \in (0.089, 0.44)$, $Ca_{ER} \in (0.69, 0.86)$, $Ca_{Mit} \in (0.38, 0.55)$ and $CaPr \in (84.4, 85.4)$.

The above time courses partially resemble the results of measurements described in [53] following histamine activation. Although in [53] not strictly oscillatory but rather calcium oscillations with vanishing amplitude tending to an equilibrium state were considered, we may

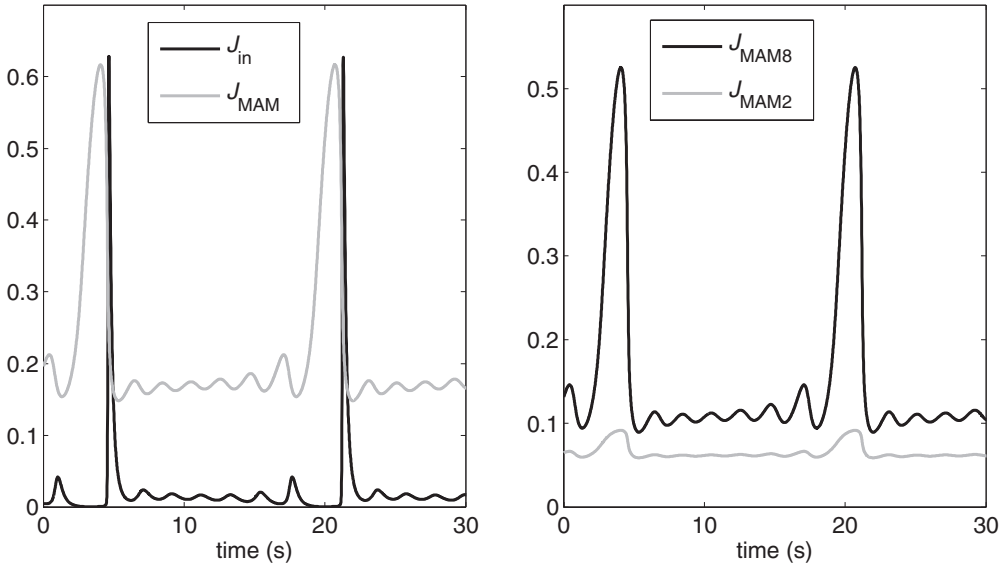


**Figure 6.** Time courses of mitochondrial calcium influxes for bursting oscillations (parameters as in table 2). Left panel $J_{in} = J_{in2} + J_{in8}$ (defined in (16)) and $J_{MAM} = J_{MAM2} + J_{MAM8}$ (defined in (17)). Right panel $J_{MAM2}$ and $J_{MAM8}$. Time integrals over one period ($T \approx 16.65$s) are $\int_t^{t+T} J_{in}(s)\,ds = 0.37$, $\int_t^{t+T} J_{MAM}(s)\,ds = 3.35$, $\int_t^{t+T} J_{MAM8}(s)\,ds = 2.47$ and $\int_t^{t+T} J_{MAM2}(s)\,ds = 1.08$.

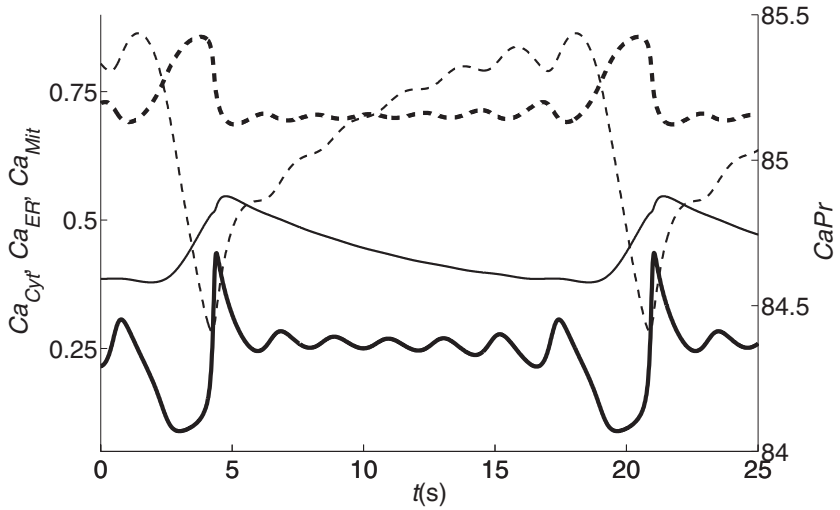


**Figure 7.** One period of bursting calcium oscillations: $Ca_{Cyt}$—thick solid line, $Ca_{Mit}$—thin solid line, $Ca_{ER}$—thick dashed line, CaPr—thin dashed line. Binding sites concentration Pr is related to CaPr by relation (7) and thus not shown here. Parameters as in table 2.

compare them with figure 7. In these experiments, calcium indicators were targeted to the intracellular compartments using indo-5F and split-YC7.3er. Thus, a rapid $Ca_{Cyt}$ increase corresponding to a reticular calcium decrease has been recorded reaching a peak after a few seconds. The peak of $Ca_{Cyt}$ preceded the peak of $Ca_{Mit}$ and the minimum of $Ca_{ER}$ concentration. A similar time sequence of concentration maxima and minima can be seen in figure 7. Another similarity is a simple non-oscillatory decrease of $Ca_{Mit}$ in contrast with small-amplitude high-frequency oscillations of $Ca_{Cyt}$ (in figure 7 between $t \cong 6$ and $t \cong 18$).

The shape and the cytosolic calcium levels in figure 7 are similar to the experimental data depicted in figure 1 in [54].

(2) *Steady states, limit cycles and impact of $k_{MAM}$ on calcium levels.*

In figure 8, we present bifurcation diagrams for $k_{MAM}$ as a bifurcation parameter and other parameters as in table 2. We have shown the bifurcation diagrams for calcium concentrations in particular compartments: $Ca_{Cyt}$ (top left), $Ca_{ER}$ (top right) and $Ca_{Mit}$ (bottom). We have found only one steady state $P$, which is unstable for $k_{MAM} \in [0, 808]$ and stable for $k_{MAM} > 808$. For $k_{MAM} = 808$, a Hopf bifurcation takes place and a stable limit cycle $LC_1$ emerges for $k_{MAM} < 808$. $LC_1$ is stable for $k_{MAM} \in [266, 808]$ and unstable for $k_{MAM} < 266$. At $k_{MAM} < 266$, a branching point of limit cycles bifurcation occurs. The unstable periodic orbit linking $LC_1$ and $LC_2$ shown in figure 8 is a hypothetical addendum

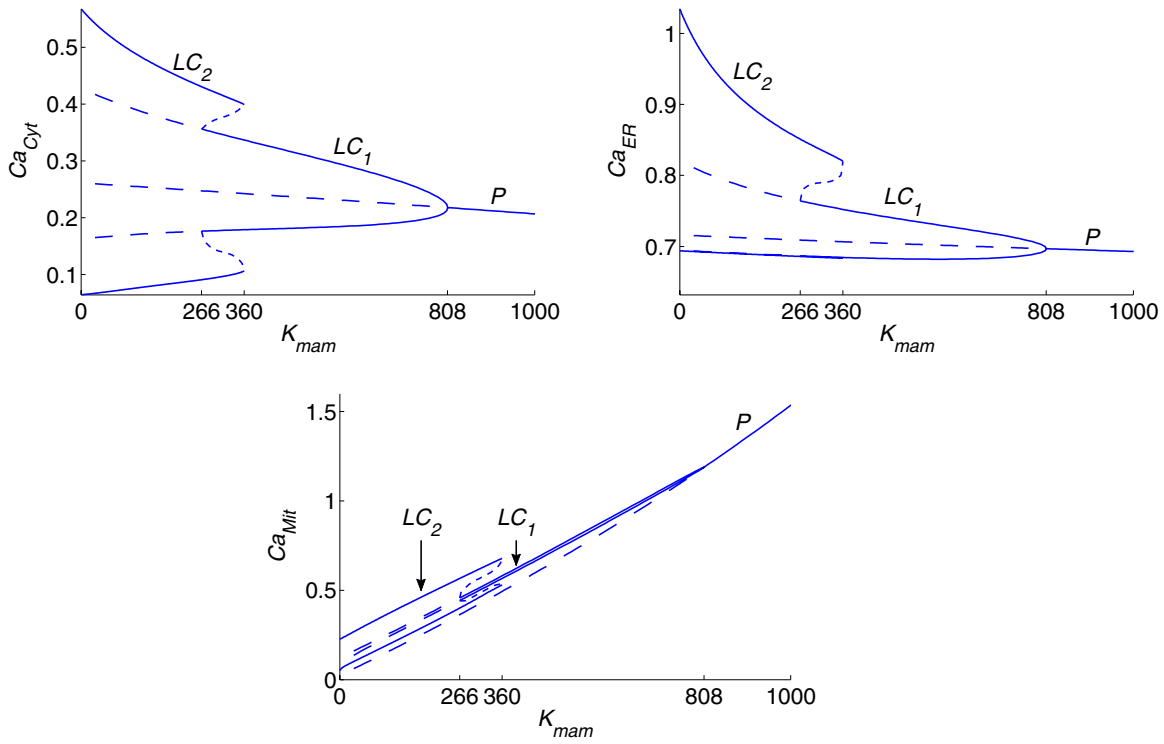


**Figure 8.** Bifurcation diagram: $Ca_{Cyt}$ (top left), $Ca_{ER}$ (top right) and $Ca_{Mit}$ (bottom) versus $k_{MAM} \in [0, 1000]$ and other parameters as in table 2. The stable stationary point exists for $k_{MAM} > 808$; at $k_{MAM} = 808$ the Hopf bifurcation occurs and a stable limit cycle $LC_1$ emerges for $k_{MAM} < 808$. $LC_1$ is unstable for $k_{MAM} < 266$. The stable limit cycle $LC_2$ exists for $k_{MAM} < 360$. Solid lines correspond to stable solutions, whereas dashed lines to unstable ones.

to the numerically found parts of the diagram. The limit cycle $LC_2$ is stable for $k_{MAM} < 360$. The solid lines denote the stable solutions, whereas the dashed lines the unstable ones.

It is seen in figure 8 that, in general, the increase of $k_{MAM}$ decreases the amplitude of oscillations and increases the minimal value of the $Ca_{Mit}$ component of the solution. The bifurcation diagram for other values of $K_{4,8}$, to which we refer in the next point 'Effect of MAMs on the period of oscillations', are qualitatively similar. The only changes are in the values of $k_{MAM}$ at which the above-mentioned bifurcations take place. For instance, for $K_{4,8} = 1.5$, the Hopf bifurcation takes place at $k_{MAM} = 238$ and the branching point-type bifurcation of limit cycle $LC_1$ occurs at $k_{MAM} = 80$.

In figure 9, we present the stable limit cycle for parameters as in table 2 and $K_3 = 3.5$ and the continuation of the stationary point $P$ with respect to $k_{MAM}$ from the interval [0, 2000]. The solid part of the continuation curve (for $k_{MAM} > 864$) corresponds to a stable steady state. The arrow indicates the direction of increasing $k_{MAM}$. The large dot represents the steady state for $k_{MAM} = 250$ (as in table 2). For $k_{MAM} > 864$, the $P$ is the only attractor of the system; hence all the trajectories tend to this stable steady state. This point is characterized by a high value of the $Ca_{Mit}$ coordinate e.g. for $k_{MAM} = 1000$ $Ca_{Mit} = 1.84$ and $k_{MAM} = 2000$ $Ca_{Mit} = 4.24$. This effect can be interpreted as an early phase of an apoptotic pathway as described below.

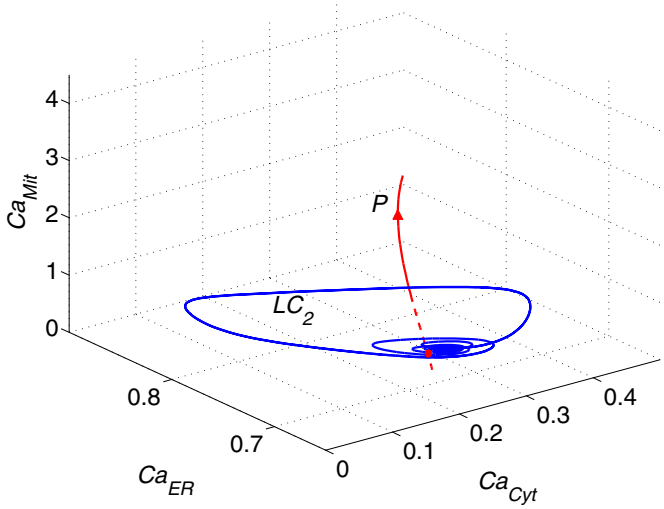


**Figure 9.** 3D phase portrait of bursting calcium oscillations for $K_3 = 3.5$ and other parameters as in table 2 and the path of the steady state for $k_{MAM} \in [0, 2000]$. Direction of increasing $k_{MAM}$ is denoted by the arrow. The dashed line corresponds to unstable steady states, while the solid line to stable ones. The Hopf bifurcation occurs at $k_{MAM} = 864$ and is denoted by a bold dot.

(3) *Effect of MAMs on the period of oscillations.*
We investigated the dependence of the period of stable oscillations on the parameters $K_{4,8}$ and $k_{MAM}$. We have confined ourselves only to stable limit cycles because unstable periodic orbits are not relevant from

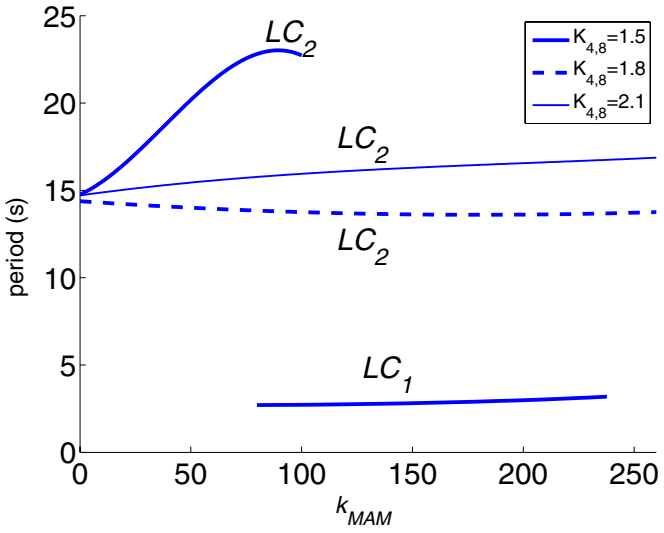


**Figure 10.** Stable oscillations period as a function of $k_{\mathrm{MAM}}$ and $K_{4,8}$, other parameters as in table 2.

the biological point of view. We have chosen $K_{4,8} = 1.5$, 1.8 and 2.1 and $k_{\mathrm{MAM}}$ in the range from 0 to 260.

The results of these computations are presented in figure 10. It is seen that for $K_{4,8} = 2.1$ the period is approximately constant and changes from 14.7 (for $k_{\mathrm{MAM}} = 0$) to 16.9 (for $k_{\mathrm{MAM}} = 260$). Similarly, for $K_{4,8} = 1.8$ the period is almost constant and decreases from 14.4 (for $k_{\mathrm{MAM}} = 0$) to 13.8 (for $k_{\mathrm{MAM}} = 260$). For these values of $K_{4,8}$, the limit cycle $\mathrm{LC}_1$ is unstable for $k_{\mathrm{MAM}} < 260$. Therefore, we have not depicted the periods of this limit cycle.

For $K_{4,8} = 1.5$ the situation is drastically different. The period of $\mathrm{LC}_2$ strongly increases from 14.8 (for $k_{\mathrm{MAM}} = 0$) to 22.7 (for $k_{\mathrm{MAM}} = 100$). For $k_{\mathrm{MAM}} \approx 100$, the period of stable oscillations drops to 2.7. This follows from the fact that close to this value of $k_{\mathrm{MAM}}$ the limit cycle $\mathrm{LC}_2$ loses its stability. The limit cycle $\mathrm{LC}_1$ exists for $k_{\mathrm{MAM}} \leqslant 238$ and is stable for $k_{\mathrm{MAM}} \geqslant 80$.

(4) *Possible apoptosis scenario.*

In physiological conditions, the major role of calcium ions in mitochondria is to stimulate ATP production through the activation of the $Ca^{2+}$-sensitive tricarboxylic acid cycle dehydrogenases [55]. However, $Ca^{2+}$ overload of the mitochondria (called mitochondrial swelling [35]) triggers opening of PTPs and finally permeabilization of the OMM. Disruption of the OMM barrier induces apoptosis by stimulating the release of apoptosis promoting factors such as cytochrome C, AIF, Smac/DIABLO or pro-caspases [51] from the perimitochondrial space to the cytoplasm, and the mitochondria transmembrane potential $\Delta\Psi_m$ collapses. Such an overload may be e.g. a result of the increase of the number of MAM complexes, implying the increase of the magnitude of $J_{\mathrm{MAM}}$ flux, which can be modelled by the increase of the $k_{\mathrm{MAM}}$ parameter.

As is suggested by experimental data, the increase of the amount of MAMs may be caused by various stress factors via the enhanced expression of proteins responsible for ER–mitochondria interface formation. For example, Park and collaborators showed in [56] that the number of calreticulin transcripts grows under a heat stress condition. Several other reticular chaperones forming MAMs, e.g. erp44, grp75, grp94, hsp90 or sigma-1 receptor (see figure 1), are upregulated by starvation, oxidative, heat or ligand induced stresses [57–59]. It is also known that exposure to an acute heat impulse leads to increased glycosylation of calreticulin [60]. Glycosylation promotes the formation of more stable complexes of chaperones, including those building MAMs [61]. Short-term stresses trigger protective response, increasing chaperones amount in the cell. However, under chronic stress conditions, mitochondria uptake large amount of $Ca^{2+}$ ions and their concentration remains elevated for a relatively long period of time, which leads to the collapse of the mitochondrial transmembrane potential ($\Delta\Psi_m$) and opening of PTPs. Rupture of mitochondrial membranes releases cytochrome C into the cytoplasm, which in turn activates caspase 9. Caspase 9 initiates the last phase of cell apoptosis resulting in the DNA fragmentation and ultimately cell death [8, 45].

Such a scenario of apoptosis can be realized in our model by increasing the $k_{\mathrm{MAM}}$ parameter. As mentioned above, we have numerically observed that for $K_3 = 3.5$ and $k_{\mathrm{MAM}} \geqslant 864$, the only attractor in the system is the stable steady state $P$ with a high $\mathrm{Ca}_{\mathrm{Mit}}$ coordinate. For example $\mathrm{Ca}_{\mathrm{Mit}} = 4.24$ for $k_{\mathrm{MAM}} = 2000$. This may be regarded as an early step of the calcium-induced apoptotic pathway (mitochondria swelling) preceding the opening of the PTPs.

We focus here only on the early steps of the calcium-induced apoptotic pathway, i.e. mitochondria swelling, before the membrane destabilization and PTPs' opening. The opening of PTPs is a kind of 'point of no-return' in the programmed death of the cell and leads to crucial physical changes inside the cell. Their modelling would require a much more complicated model than the presented one. Thus, the calcium efflux through PTPs and the subsequent changes have been omitted in this paper.

Similar results (protracted increased mitochondrial calcium level) can be obtained in this model by reducing significantly the calcium efflux from mitochondria, keeping the mitochondrial calcium uptake ($J_{\mathrm{MAM}}$ and $J_{\mathrm{in}}$) at the same level. Such an effect can be obtained either by reducing the coefficient $k_{\mathrm{out}}$ or by increasing the mNCX half-activation constant $K_3$. However, such changes seem to have less biological background than increasing $K_{\mathrm{MAM}}$, because attenuation of $J_{\mathrm{out}}$ is observed only in non-physiological conditions caused e.g. by treatment with benzothiazepin compounds or NCX expression blocking. Specifically, it was demonstrated that the CGP-37157 compound was able to trigger the mitochondrial $Ca^{2+}$ rise by blocking the exchanger thereby leading to enhanced mitochondrial oxidative metabolism and insulin secretion [62]. This effect could also be obtained using siRNA construct, which has a blocking effect on the endogenous exchanger activity [63].

**Remark 1.** As can be seen from figures 4, 5 and 7, the levels of free calcium ions in all of the compartments attain values between 0.1 and 1 $\mu$M. In the case of the cytosolic calcium level this is a biologically acceptable range of values, whereas in the case of ER and mitochondria such values of calcium concentration are far too small, and in the case of ER it is about two orders of magnitude less than that found in reality [2, 64]. Similar incongruities are, however, present in other models [19, 65, 54]. These apparent incompatibilities can be explained by the assumption that the calcium concentrations in ER and mitochondria in these models, as well as in the model presented in this paper, are measured from some fixed sufficiently large constant levels $Ca_{ER0}$ and $Ca_{Mit0}$, which can be regarded as reference levels.

## 5. Conclusions

We have proposed a new model of intracellular calcium oscillations, which explicitly takes into account the existence of mitochondria-associated ER membrane complexes (MAMs)—the connection sites between endoplasmic reticulum (ER) and mitochondria. The model is a modification of the model introduced in [19]. The modification consists in introducing a straightforward flow of calcium ions between ER and mitochondria, as well as in a different form of the calcium flux from the mitochondria to the cytosol. In [19], this flow depends on the cytosolic concentration of free calcium $Ca_{Cyt}$ and is assumed in the form $J_{out} = k_{out}\left(\frac{Ca^2_{Cyt}}{K_3^2+Ca^2_{Cyt}} + k_m\right)Ca_{Mit}$, where $k_m$ is a constant. The form of $J_{out}$ is based on [42, 66] and references therein. In this paper, the speed of the outflow from mitochondria determined by (15) depends only on $Ca_{Mit}$. This is an essential modification which seems to exclude the possibility of chaotic oscillations which occur in the Marhl model, because such oscillations have not appeared in our numerical findings.

We have examined numerically the influence of MAMs on the period and shape of calcium oscillations. The obtained oscillations have a bursting character. We have examined the dependence of the period of oscillatory solutions on the parameter $k_{MAM}$. Interestingly, we have found that for $k_{MAM}$ from certain interval (depending on the value of $K_{4,8}$) there coexist two stable limit cycles differing from each other in amplitude and period. The second limit cycle, which has a smaller amplitude and smaller period, becomes stable for sufficiently large $k_{MAM}$. Finally, for sufficiently large $k_{MAM}$ oscillations disappear and the majority of trajectories are attracted by the stable steady state $P$ with a high calcium level in mitochondria (see figure 9). This can be interpreted as an early step in an apoptotic pathway. The proposed, biologically reasonable, potential scenario of early steps in an apoptotic pathway is strictly connected with the MAM complexes.

## Acknowledgments

The authors would like to thank the referees for their valuable comments and suggestions. This work was supported by the FNP project TEAM/2009-3/6 'Mechanistic aspects and spatial organization of cell signaling' (MD) and by MNiSW grants N N201548738 (BK), and N N201 547638 (PS).

## References

[1] Clapham D E 2007 Calcium signaling *Cell* **131** 1047–58
[2] Laude A J and Simpson A W M 2009 Compartmentalized signalling: $Ca^{2+}$ compartments, microdomains and the many facets of $Ca^{2+}$ signalling *FEBS J.* **276** 1800–16
[3] Montell C 2005 The latest waves in calcium signaling *Cell* **122** 157–63
[4] Oster A M, Thomas B, Terman D and Fall C P 2011 The low conductance mitochondrial permeability transition pore confers excitability and CICR wave propagation in a computational model *J. Theor. Biol.* **273** 216–31
[5] Pfeiffer D R, Gunter T E, Eliseev R, Broekemeier K M and Gunter K K 2001 Release of $Ca^{2+}$ from mitochondria via the saturable mechanisms and the permeability transition *IUBMB Life* **52** 205–12
[6] Chipuk J E, Bouchier-Hayes L and Green D R 2006 Mitochondrial outer membrane permeabilization during apoptosis: the innocent bystander scenario *Cell Death Differ.* **13** 1396–402
[7] Tait S W, Parsons M J, Llambi F, Bouchier-Hayes L, Connell S, Munoz-Pinedo C and Green D R 2010 Resistance to caspase-independent cell death requires persistence of intact mitochondria *Dev. Cell* **18** 802–13
[8] Hajnóczky G, Csordás G, Das S, Garcia-Perez C, Saotome M, Roy S S and Yi M 2006 Mitochondrial calcium signaling and cell death: approaches for assessing the role of mitochondrial $Ca^{2+}$ uptake in apoptosis *Cell Calcium* **40** 553–60
[9] Dennis E A and Kennedy E P 1972 Intracellular sites of lipid synthesis and the biogenesis of mitochondria *J. Lipid Res.* **13** 263–7
[10] Rusinol A E, Cui Z, Chen M H and Vance J E 1994 A unique mitochondria-associated membrane fraction from rat liver has a high capacity for lipid synthesis and contains pre-golgi secretory proteins including nascent lipoproteins *J. Biol. Chem.* **269** 27494–502
[11] Giorgi C, De Stefani D, Bononi A, Rizzuto R and Pinton P 2009 Structural and functional link between the mitochondrial network and the endoplasmic reticulum *Int. J. Biochem. Cell Biol.* **41** 1817–27
[12] Lebiedzinska M, Szabadkai G, Jones A W E, Duszynski J and Wieckowski M R 2009 Interactions between the endoplasmic reticulum, mitochondria, plasma membrane and other subcellular organelles *Int. J. Biochem. Cell Biol.* **41** 1805–16
[13] Csordás G, Renken C, Várnai P, Walter L, Weaver D, Buttle K F, Balla T, Mannella C A and Hajnóczky G 2006 Structural and functional features and significance of the physical linkage between ER and mitochondria *J. Cell Biol.* **174** 915–21
[14] Hayashi T, Rizzuto R, Hajnóczky G and Su T-P 2009 MAM: more than just a housekeeper *Trends Cell Biol.* **19** 81–88
[15] Csordás G, Várnai P, Golenár T, Roy S, Purkins G, Schneider T G, Balla T and Hajnóczky G 2010 Imaging interorganelle contacts and local calcium dynamics at the ER-mitochondrial interface *Mol. Cell* **39** 121–32
[16] Giacomello M, Drago I, Bortolozzi M, Scorzeto M, Gianelle A, Pizzo P and Pozzan T 2010 $Ca^{2+}$ hot spots on the mitochondrial surface are generated by $Ca^{2+}$ mobilization from stores, but not by activation of store-operated $Ca^{2+}$ channels *Mol. Cell* **38** 280–90
[17] Keener J and Sneyd J 1998 *Mathematical Physiology* (New York: Springer)

[18] Marhl M, Schuster S and Brumen M 1998 Mitochondria as an important factor in the maintenance of constant amplitudes of cytosolic calcium oscillations *Biophys. Chem.* **71** 125–32

[19] Marhl M, Haberichter T, Brumen M and Heinrich R 2000 Complex calcium oscillations and the role of mitochondria and cytosolic proteins *Biosystems* **57** 75–86

[20] Schuster S, Marhl M and Höfer T 2002 Modelling of simple and complex calcium oscillations. From single-cell responses to intercellular signalling *Eur. J. Biochem.* **269** 1333–55

[21] Hariprasad D, McNulty M, Shi J and Tian P 2009 Three-pool model of calcium signaling http://jxshix.people.wm.edu/research-students.html

[22] Hajnóczky G, Csordás G, Madesh M and Pacher P 2000 The machinery of local $Ca^{2+}$ signalling between sarco-endoplasmic reticulum and mitochondria *J. Physiol.* **529** 69–81

[23] Coe H and Michalak M 2009 Calcium binding chaperones of the endoplasmic reticulum *Gen. Physiol. Biophys.* **28** F96–103

[24] Schwaller B 2010 Cytosolic $Ca^{2+}$ buffers *Cold Spring Harb. Perspect. Biol.* **2** a004051

[25] Parekh A B 2003 Mitochondrial regulation of intracellular $Ca^{2+}$ signaling: more than just simple $Ca^{2+}$ buffers *News Physiol. Sci.* **18** 252–6

[26] Falcke M 2004 Reading the patterns in living cells—the physics of $Ca^{2+}$ signaling *Adv. Phys.* **53** 255–440

[27] Sparagna G C, Gunter K K, Sheu S-S and Gunter T E 1995 Mitochondrial calcium uptake from physiological-type pulses of calcium *J. Biol. Chem.* **270** 27510–5

[28] Bazil J N and Dash R K 2011 A minimal model for the mitochondrial rapid mode of $Ca^{2+}$ uptake mechanism *PLoS One* **6** e21324

[29] Jouaville L S, Ichas F, Holmuhamedov E L, Camacho P and Lechleiter J D 1995 Synchronization of calcium waves by mitochondrial substrates in *Xenopus leavis* oocytes *Nature* **377** 438–441

[30] Hehl S, Golard A and Hille B 1996 Involvement of mitochondria in intracellular calcium sequestration by rat gonadotropes *Cell Calcium* **20** 515–24

[31] Hoth M, Fanger C M and Lewis R S 1997 Mitochondrial regulation of store-operated calcium signalling in T lymphocytes *J. Cell Biol.* **137** 633–48

[32] Ricken S, Leipziger J, Greger R and Nitschke R 1998 Simultaneous measurements of cytosolic and mitochondrial $Ca^{2+}$ transients in HT29 cells *J. Biol. Chem.* **273** 34961–9

[33] Skupin A and Falcke M 2009 From puffs to global $Ca^{2+}$ signals: how molecular properties shape global signals *Chaos* **19** 037111

[34] Hoogenboom B W, Suda K, Engel A and Fotiadis D 2007 The supramolecular assemblies of voltage-dependent anion channels in the native membrane *J. Mol. Biol.* **370** 246–55

[35] Shoshan-Barmatz V, De Pinto V, Zweckstetter M, Raviv Z, Keinan N and Arbel N 2010 VDAC, a multi-functional mitochondrial protein regulating cell life and death *Mol. Asp. Med.* **31** 227–85

[36] Dupont G and Combettes L 2009 What can we learn from the irregularity of $Ca^{2+}$ oscillations? *Chaos* **19** 037112

[37] Wagner J and Keizer J 1994 Effects of rapid buffers on $Ca^{2+}$ diffusion and $Ca^{2+}$ oscillations *Biophys. J.* **67** 447–56

[38] Dawson A P, Rich G T and Loomis-Husselbee J W 1995 Estimation of the free $[Ca^{2+}]$ gradient across endoplasmic reticulum membranes by a null-point method *Biochem. J.* **310** 371–4

[39] Li Y X, Keizer J, Stojilkovic S S and Rinzel J 1995 Calcium excitability of the ER membrane: an explanation for IP3-induced $Ca^{2+}$ oscillations *Am. J. Physiol. Cell Physiol.* **269** C1079–92

[40] Sneyd J, Tsaneva-Atanasova K, Yule D I, Thompson J L and Shuttleworth T J 2004 Control of calcium oscillations by membrane fluxes *Proc. Natl Acad. Sci. USA* **101** 1392–6

[41] Babcock D F and Hille B 1998 Mitochondrial oversight of cellular $Ca^{2+}$ signaling *Curr. Opin. Neurobiol.* **8** 398–404

[42] Mazel T, Raymond R, Raymond-Stintz M, Jett S and Wilson B S 2009 Stochastic modeling of calcium in 3D geometry *Biophys J.* **96** 1691–706

[43] Babcock D F, Herrington J, Goodwin P C, Park Y B and Hille B 1997 Mitochondrial participation in the intracellular $Ca^{2+}$ network *J. Cell Biol.* **136** 833–44

[44] Starkov A A 2010 The molecular identity of the mitochondrial $Ca^{2+}$ sequestration system *FEBS J.* **277** 3652–63

[45] Rasola A and Bernardi P 2007 The mitochondrial permeability transition pore and its involvement in cell death and in disease pathogenesis *Apoptosis* **12** 815–33

[46] Gunter T E and Sheu S 2009 Characteristics and possible functions of mitochondrial $Ca^{2+}$ transport mechanisms *Biochim. Biophys. Acta* **1787** 1291–308

[47] Marhl M, Schuster S, Brumen M and Heinrich R 1997 Modeling the interrelations between the calcium oscillations and ER membrane potential oscillations *Biophys. Chem.* **63** 221–39

[48] Chepyzov V V and Vishik M I 2002 *Attractors for Equations of Mathematical Physics* (Providence, RI: American Mathematical Society)

[49] Govaerts W and Kuznetsov Y A www.matcont.ugent.be

[50] Joseph S K and Hajnóczky G 2007 $IP_3$ receptors in cell survival and apoptosis: $Ca^{2+}$ release and beyond *Apoptosis* **12** 951–68

[51] Roy S S and Hajnóczky G 2008 Calcium, mitochondria and apoptosis studied by fluorescence measurements *Methods* **46** 213–23

[52] Rizzuto R, Pinton P, Ferrari D, Chami M, Szabadkai G, Magalhães P J, Di Virgilio F and Pozzan T 2003 Calcium and apoptosis: facts and hypotheses *Oncogene* **22** 8619–27

[53] Ishii K, Hirose K and Iino M 2006 $Ca^{2+}$ shuttling between endoplasmic reticulum and mitochondria underlying $Ca^{2+}$ oscillations *EMBO Rep.* **7** 390–6

[54] Borghans J M, Dupont G and Goldbeter A 1997 Complex intracellular calcium oscillations. A theoretical exploration of possible mechanisms *Biophys. Chem.* **66** 25–41

[55] McCormack J G and Denton R M 1989 The role of $Ca^{2+}$ ions in the regulation of intramitochondrial metabolism and energy production in rat heart *Mol. Cell Biochem.* **89** 121–5

[56] Park B J *et al* 2001 Calreticulin, a calcium-binding molecular chaperone, is required for stress response and fertility in *Caenorhabditis elegans* *Mol. Biol. Cell* **12** 2835–45

[57] Ellgaard L and Helenius A 2001 ER quality control: towards an understanding at the molecular level *Curr. Opin. Cell Biol.* **13** 431–7

[58] Anelli T, Alessio M, Mezghrani A, Simmen T, Talamo F, Bachi A and Sitia R 2002 ERp44, a novel endoplasmic reticulum folding assistant of the thioredoxin family *EMBO J.* **21** 835–44

[59] Hayashi T and Su T P 2007 Sigma-1 receptor chaperones at the ER-mitochondrion interface regulate $Ca^{2+}$ signaling and cell survival *Cell* **131** 596–610

[60] Jethmalani S M and Henle K J 1998 Calreticulin associates with stress proteins: implications for chaperone function during heat stress *J. Cell Biochem.* **69** 30–43

[61] Mizzen L A, Kabiling A N and Welch W J 1991 The two mammalian mitochondrial stress proteins, grp 75 and hsp 58, transiently interact with newly synthesized mitochondrial proteins *Cell Regul.* **2** 165–79

[62] Lee B *et al* 2003 Inhibition of mitochondrial $Na^+$–$Ca^{2+}$ exchanger increases mitochondrial metabolism and potentiates glucose-stimulated insulin secretion in rat pancreatic islets *Diabetes* **52** 965–73

[63] Nita I I *et al* 2012 The mitochondrial $Na^+/Ca^{2+}$ exchanger upregulates glucose dependent $Ca^{2+}$ signalling linked to insulin secretion *PLoS One* **7** e46649

[64] Sneyd J 2005 Modeling $IP_3$-dependent calcium dynamics in non-excitable cells *Tutorials in Mathematical Biosiences II: Mathematical Modeling of Calcium Dynamics and Signal Transduction* ed J Sneyd (Berlin: Springer)

[65] Goldbeter A, Dupont G and Berridge M J 1990 Minimal model for signal-induced $Ca^{2+}$ oscillations and for their frequency encoding through protein phosphorylation *Proc. Natl Acad. Sci. USA* **87** 1461–5

[66] Magnus G and Keizer J 1997 Minimal model of beta-cell mitochondrial $Ca^{2+}$ handling *Am. J. Physiol.* **273** C717–33